Vol 17 No 6, June 2008
1674-1056/2008/17(06)/2027-06

Chinese Physics B

© 2008 Chin. Phys. Soc.
and IOP Publishing Ltd

Relativistic multichannel treatment of autoionization Rydberg series of $4s^2nf(n = 4 - 23)J^\pi = (7/2)^\circ$ for scandium*

Jia Feng-Dong(贾凤东), Wang Jing-Yang(王京阳), and Zhong Zhi-Ping(钟志萍)†

College of Physical Sciences, Graduate University of the Chinese Academy of Sciences, PO Box 4588, Beijing 100049, *China*

(Received 10 October 2007; revised manuscript received 7 November 2007)

Based on relativistic multichannel theory, this paper calculates the energy levels of autoionization Rydberg series $4s^2nf(n = 4 - 23)J^\pi = (7/2)^\circ$ of scandium at different levels of approximation within the framework of multichannel quantum defect theory. The present results show that the dipole polarizations play an important role. Considering the dynamical dipole polarization effects, this paper finds that the difference between calculated and experimental quantum defects for the $4s^2nf(n = 4 - 23)J^\pi = (7/2)^\circ$ series is generally about 0.01–0.03. Furthermore, the reason that $4s^216f$ is obscured in experimental spectra is suggested to be the interaction with the neighbouring resonance state converged to $3d^2(^1G_4)$ of Sc^+.

Keywords: relativistic multichannel theory, multichannel quantum defect theory, electron–electron correlations

PACC: 3120, 3120A, 3120T

1. Introduction

The investigation of electron–electron correlations of atoms is a significant subject in modern physics research. Atomic scandium (Sc) has three valence electrons and is the simplest open-shell atom with a partially filled d subshell, and can show complex spectra.[1] In fact, as shown in Table 1, the first 13 levels of Sc^+ have a spread of only 14 000 cm^{-1} −1.7 eV;[2] the small spread is partly due to the near degeneracy of the 4s and 3d orbitals.[3] Consequently, there are rich and complex energy structures especially close to the first ionization threshold. Therefore, Sc can be employed to demonstrate rich electron–electron correlation effects. In addition, rare earth element is now widely used in material industry,[4,5] understanding of the electronic structure of rare earth element would benefit the applications in relative industries. As the simplest rare earth element, the lessons leaned from scandium may apply to other transition metals since the valence shells for all these atoms include both s and d orbitals.[3] These make scandium especially attractive from both theoretical and experimental point of view.

Table 1. Experimental Sc^+ energy levels.[2]

Config.	Term	J	Energy/cm^{-1}
3d4s	^3D	1	0
	^3D	2	67.72
	^3D	3	177.76
3d4s	^1D	2	2540.95
$3d^2$	^3F	2	4802.87
		3	4883.57
		4	4987.79
$3d^2$	^1D	2	10944.56
$4s^2$	^1S	0	11736.36
$3d^2$	^3P	0	12074.10
		1	12101.50
		2	12154.42
$3d^2$	^1G	4	14261.32
$3d^2$	^1S	0	25955.2
3d4p	...	...	...
4s4p	^3P	0	39002.20
		1	39115.04
		2	39345.52
4s4p	^1P	1	55715.36

*Project supported by the National Natural Science Foundation of China (Grant No 10574162) and partial supported from the Scientific Research Fund of GUCAS (Grant No 055101BM03).

†Corresponding author. E-mail: zpzhong@gucas.ac.cn

Here, we take the autoionization Rydberg series $4s^2nf(n = 4 - 23)J^\pi = (7/2)^\circ$ of scandium as an example to elucidate electron–electron correlation effects of atomic scandium. Experimentally, the absorption spectrum of scandium has been photographed in the spectral range 120–320 nm.[6] The autoionization Rydberg series $4s^2nf(n = 4 - 23)J^\pi = (7/2)^\circ$ are identified as well as other seven Rydberg and autoionization series. Theoretically, Greene *et al*[3] calculated the photoionization cross section of Sc from the $3d4s^2(^2D_{3/2,5/2})$ ground electronic state using eigenchannel R-matrix calculations. It should be noted that the techniques employed by Greene *et al*[3] are 'nearly' *ab initio*, i.e. the effects of the 18 core electrons are described using a screened Coulomb potential[7,8] with a dipole polarizability, and spin-orbit effects are incorporated through the $LS - jj$ frame transformation.[9,10] As for the $4s^2nf(n = 4-23)J^\pi = (7/2)^\circ$ series, the difference between the calculated quantum defects by Greene *et al*[3] and experimental quantum defects[6] was less than 0.02 for $n = 4 - 15$ with the exception of $n = 13$, and the difference for $n = 16 - 23$ was larger than 0.05. The relationship between the excited orbital energy ε_i and the eigenchannel quantum defect μ_i is shown in the following formula. Noted that all these formulas in this paper are written in atomic units.

$$\varepsilon_i = -\frac{1}{2}\nu_i^2, \tag{1}$$

here $\nu_i = n-\mu_i$ is the effective quantum number of the ith channel, μ_i is the quantum defect for eigenchannel i.

In this paper, based on relativistic multichannel theory which is a completely *ab initio* and fully relativistic non-perturbative theory, we calculated energy levels of $4s^2nf(n = 4 - 23)J^\pi = (7/2)^\circ$ series at different levels of approximation, i.e., electron–electron correlations have been treated by configuration interactions through choosing appropriate channels. Our results show that the dipole polarizations play an important role on this autoionization Rydberg series $4s^2nf(n = 4 - 23)J^\pi = (7/2)^\circ$. Considering the dynamical dipole polarization effects, we find that the difference between calculated and experimental quantum defects[6] for this series is generally about 0.01–0.03 for $n = 4-23$ with the exception of $n = 20, 22, 23$. Furthermore, the reason that $4s^216f$ is obscured in experimental spectra is suggested to be the interaction with the neighbouring resonance state converged to $3d^2(^1G_4)$of Sc^+.

2. Theoretical method

Within the framework of multichannel quantum defect theory (MQDT),[10−14] infinite Rydberg orbitals and adjacent continua orbitals can be treated in a unified manner through a compact set of physical parameters (e.g., eigenchannel quantum defects μ_α and transformation matrices $U_{i\alpha}$). Usually, MQDT parameters $(\mu_\alpha, U_{i\alpha})$ are determined semi-empirically by fitting accurate energy levels into spectroscopic data or by the first principle calculations. Relativistic multichannel theory (RMCT) can be regarded as an extension of the traditional configuration interaction method by including the continuum configuration interactions.[15−20] It aims directly to calculate the MQDT parameters $(\mu_\alpha, U_{i\alpha})$ and has been used to calculate energy levels, Landé g factors, and the coupling scheme within the framework of the MQDT method.[16−21]

In the framework of the relativistic channel theory, a relativistic atomic Hamiltonian is written as

$$\begin{aligned} H &= \sum_i \left(c\alpha_i \cdot p_i + \beta_i mc^2 - \frac{Ze^2}{r_i} \right) + \sum_{i>j} \frac{e^2}{r_{ij}} \\ &= H_0 + V. \end{aligned} \tag{2}$$

A relativistic atomic self-consistent Hamiltonian H_0 can be obtained by an atomic self-consistent field (SCF) calculation such as Dirac–Slater SCF with a local exchange approximation,[22,23]

$$\begin{aligned} H_0 &= \sum_i h_i \\ &= \sum_i [(c\alpha_i \cdot p_i) + \beta_i mc^2 + V_{\mathrm{SCF}}(r_i)], \end{aligned} \tag{3}$$

and a residual interaction V is defined as

$$V = \sum_i \left[-\frac{Ze^2}{r_i} - V_{\mathrm{SCF}}(r_i) \right] + \sum_{i>j} \frac{e^2}{r_{ij}}. \tag{4}$$

Based on V_{SCF}, we can calculate all bound and unbound single-electron wavefunctions φ_a with combined quantum numbers $a = nk$ or εk. From such a complete set of single-electron wavefunctions (i.e. orbitals), we construct bound and continuum configuration wavefunctions (Φ_n or $\Phi_{i\varepsilon}$) as antisymmetrized product-type wavefunctions of N single-electron wavefunctions with electron occupation distributions and appropriate angular momentum couplings. N-electron wavefunctions can be expressed

as:[15−20]

$$\Psi(E,i) = \sum_n A_n(E,i)\,\Phi_n + \sum_j \int_{\varepsilon_c} B_{j\varepsilon}(E,i)\,\Phi_{j\varepsilon}\cdot \mathrm{d}\varepsilon. \quad (5)$$

The index j refers to various ionization channels which are various classes of configuration wavefunctions (Φ_n or $\Phi_{i\varepsilon}$) with the same core state and different radial excited orbitals (φ_{nk} or $\varphi_{\varepsilon k}$) with similar angular momentum couplings, and the energy integration can be treated by appropriate energy messages and starts from ε_c(decided according to convenience of computation) above which infinite Rydberg-type configuration functions are treated as channels. The coefficients $A_n(E,i)$ and $B_{i\varepsilon}(E,i)$ in Eq.(5) can be expressed in terms of a K matrix.[15−20]

$$A_n(E,i) = \frac{K_{n,iE}}{E-E_n^{\circ}}\cdot D(E,i), \quad (6)$$

$$B_{j\varepsilon}(E,i) = \left[P\frac{K_{j\varepsilon,iE}}{(E-\varepsilon)} + \delta_{ji}\cdot\delta(\varepsilon-E)\right]\cdot N(E,i). \quad (7)$$

With the calculated matrix elements of residual interactions $V_{n,n'}$, $V_{n,j\varepsilon}$, $V_{j\varepsilon,j'\varepsilon'}$ (representing discrete–discrete, discrete–continuum, continuum–continuum interactions respectively), it then leads to Lippmann–Schwinger integral equations of the K matrix,

$$K_{n',iE} = V_{n',iE} + \sum_j \int_{\varepsilon_c} \frac{V_{n',j\varepsilon}K_{j\varepsilon,iE}}{E-\varepsilon}\mathrm{d}\varepsilon + \sum_n \frac{V_{n',n}K_{n,iE}}{E-E_n^0}, \quad (8)$$

$$K_{j'\varepsilon',iE} = V_{j'\varepsilon',iE} + \sum_j \int_{\varepsilon_c} \frac{V_{j'\varepsilon',j\varepsilon}K_{j\varepsilon,iE}}{E-\varepsilon}\mathrm{d}\varepsilon + \sum_n \frac{V_{j'\varepsilon',n}K_{n,iE}}{E-E_n^0}, \quad (9)$$

where $E_{kn}^0 = E_{kc}^0 + \varepsilon_n$ and E_{kc}^0 are the energies of various relevant ionic cores. After solving the integral equation, the physical parameters (eigenchannel quantum defects μ_α, and transformation matrix $U_{i\alpha}$) in MQDT can be obtained directly, just by diagonalizing the K matrix on energy shell.[15−20]

For the closed dissociation channels, the orbital energy $\varepsilon_i = -\dfrac{1}{2\nu_i} < 0$, the excitation energy ε in the autoionization region can be expressed in terms of ν_i:

$$\varepsilon = I_i + \varepsilon_i = I_i - \frac{1}{2\nu_i^2}, \quad (10)$$

where I_i represents the ith autoionization threshold. With a specified energy ε which lies in continua energy levels, we can obtain the corresponding ν_i for ith dissociation channel from Eq.(10).

3. Result and discussion

Based on RMCT, we calculated energy levels of autoionization Rydberg series $4s^2nf(n=4-23)J^\pi = (7/2)^\circ$ of scandium at different levels of approximation.

Starting with the relativistic self-consistent Hamiltonian in Eq.(3), we calculate the self-consistent quantum defects μ_1 of $4s^2nf(n=4-23)J^\pi = (7/2)^\circ$ series. As shown in Fig.1, the self-consistent quantum defects μ_1 of $4s^2nf$ $J^\pi = (7/2)^\circ$ series change slowly and smoothly near the ionization threshold of $4s^2$, which reflects the accuracy of our calculations. Noted that these calculated self-consistent quantum defects are much smaller than the experimental data, the difference is more than 0.1 as shown in Table 2. The experimental quantum defects μ_{EXP} are obtained from experimental energy levels[2] and Eq.(10). Noted that the $4s^216f$ is obscured in experimental spectra, we will discuss the reason later.

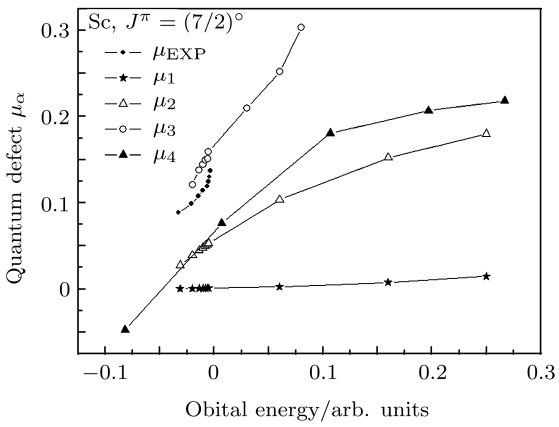


Fig.1. The quantum defects of the $4s^2nf(n=4-23)J^\pi = (7/2)^\circ$ series as the function of energy, $E=0$ corresponds to the ionization threshold of $4s^2(^1S)$ of scandium. μ_1 are self-consistent quantum defects; μ_2 are eigenchannel quantum defects obtained by FCA; μ_3 are eigenchannel quantum defects obtained by considering dipole polarization effects; μ_4 are quantum defects obtained from the energy levels calculated by considering the effects of the first 14 levels of Sc^+ and Eq.(10); μ_{EXP} are experimental quantum defects obtained from experimental energy levels[2] and Eq.(10) with the ionization threshold of $4s^2$ of scandium.

In order to treat the electron–electron correlations more precisely, we first just considered the configuration interactions in a single channel $(4s^2, {}^1S)_0^+(\varphi_{nf7/2}, \varphi_{\varepsilon f7/2})$, which means that the ionic core state $4s^2$ of our target series is 'frozen', does not be changed by excited electron, i.e., it is so called 'frozen core approximation (FCA)'. As shown in Fig.1, the eigenchannel quantum defects μ_2 of $4s^2nf$ $J^\pi = (7/2)^\circ$ series calculated by FCA also change slowly and smoothly near the ionization threshold of $4s^2$, which reflects the accuracy of our calculations. In the energy region of interest, the FCA quantum defects μ_2 are larger than μ_1 as shown in Fig.1. However, the difference between μ_2 and $\mu_{\rm EXP}$ is still generally about 0.08 as shown in Table 2.

Table 2. The comparison of quantum defects of $4s^2nf(n = 4-23)J^\pi = (7/2)^\circ$ between experimental and calculated by different levels of approximation, and energy levels of experimental $E_{\rm EXP}$ and calculated E_3 obtained by considering dipole polarization effects.

n	$E^{[2]}_{\rm EXP}/{\rm cm}^{-1}$	$E_3/{\rm cm}^{-1}$	$\Delta\mu_1^*$	$\Delta\mu_2^*$	$\Delta\mu_3^*$	$\Delta\mu_4^*$
4	57485.7	57456.3	0.10	0.06	-0.01	0.07
5	60090.4	60047.7	0.10	0.06	–0.02	0.05
6	61498.0	61468.1	0.12	0.06	–0.03	0.08
7	62343.8	62324.3	0.13	0.07	–0.03	0.08
8	62886.2	62878.2	0.13	0.08	–0.02	0.09
9	63267.0	63257.0	0.12	0.07	–0.03	0.08
10	63533.2	63525.5	0.13	0.07	–0.03	0.08
11	63729.6	63724.4	0.13	0.08	–0.03	0.04
12	63878.6	63875.4	0.14	0.08	–0.02	0.09
13	63993.8	63992.5	0.15	0.10	–0.01	0.05
14	64086.2	64085.2	0.15	0.10	–0.01	0.06
15	64160.4	64159.8	0.15	0.10	–0.01	0.12
16	Obscured	64220.1				
17	64271.2	64271.2	0.16	0.11	0.00	0.09
18	64312.4	64313.4	0.19	0.14	0.02	0.12
19	64348.0	64349.0	0.20	0.14	0.03	0.13
20	64378.3	64379.4	0.21	0.15	0.04	0.19
21	64404.8	64405.6	0.20	0.14	0.03	0.14
22	64426.6	64428.2	0.24	0.19	0.07	0.18
23	64445.8	64447.9	0.28	0.22	0.11	0.23

*$\Delta\mu_i = \mu_{\rm EXP} - \mu_i$, μ_1 are self-consistent quantum defects; μ_2 are eigenchannel quantum defects obtained by FCA; μ_3 are eigenchannel quantum defects obtained by considering dipole polarization effects; μ_4 are quantum defects obtained from the energy levels calculated by considering the effects of the first 14 levels of Sc^+ and Eq.(10).

Furthermore, the other ionization channels with excited-state cores and appropriate excited orbitals will be important for electron–electron correlations, such as dynamical polarizations.[18,19] Dynamical polarizations mean that the ionic core is polarized by excited electron, i.e., result in the $|\Delta l| = 1, 2, \cdots$, here l is the angular quantum number of ionic core. $|\Delta l| = 1$ is called dipole polarization, $|\Delta l| = 2$ is called quadrupole polarization, etc. As an example of ionic core $4s^2$ in this work, $|\Delta l| = 1$ corresponds to 4s4p, $\cdots$; $|\Delta l| = 2$ corresponds to 4s3d, 4s4d, $\cdots$. For $4s^2nf(n = 4 - 23)J^\pi = (7/2)^\circ$, there are four channels with the ionic core 4s4p related to dipole polarization effects: (4s4p, ${}^1P)_1^+(\varphi_{nf5/2}, \varphi_{\varepsilon f5/2})$, (4s4p, ${}^3P)_1^-(\varphi_{nf5/2}, \varphi_{\varepsilon f5/2})$, (4s4p, ${}^3P)_2^-(\varphi_{nf3/2}, \varphi_{\varepsilon f3/2})$, (4s4p, ${}^3P)_2^-(\varphi_{nf5/2}, \varphi_{\varepsilon f5/2})$. Noted that, these four channels are strongly closed channels, i.e., their precursor states are far above the energy region of $4s^2nf(n = 4 - 23)J^\pi = (7/2)^\circ$ series, thus there is only one dissociation physical channel $(4s^2, {}^1S)_0^+(\varphi_{nf7/2}, \varphi_{\varepsilon f7/2})$ below the ionization threshold $4s^2({}^1S)$. Considering the dipole polarization effects, we find that the eigenchannel quantum defects μ_3 of $4s^2nfJ^\pi = (7/2)^\circ$ series also change

slowly and smoothly near the ionization threshold of $4s^2$, which reflects the accuracy of our calculations and is shown in Fig.1. In the energy region of interest, eigenchannel quantum defects μ_3 is larger than the eigenquantum defect μ_2 obtained from FCA as shown in Fig.1. And μ_3 is in good agreement with the experimental results $\mu_{\rm EXP}$, more specifically, the difference between them is generally about 0.01–0.03 with the exception of $n = 20, 22, 23$ as shown in Table 2. When n is larger than 20, the difference of quantum defect is 0.04 for $n = 20$, 0.07 for $n = 22$, and 0.11 for $n = 23$ respectively. The reason that difference becomes larger for high $n \geq 20$ is discussed as follows: based on Eq.(1), one can get $\Delta\mu = \Delta E(n-\mu)^3$. Here $\Delta\mu$ is the difference of experimental and calculated quantum defects, ΔE is the difference of experimental and calculated energy level correspondingly, μ is the quantum defects. Therefore, the error in the quantum defect increases rapidly as n gets large even if there is a small error in energy level. For example, when n equals 23, a small error in energy level about $1\,{\rm cm}^{-1}$ results in a error in quantum defects about 0.05, while as $n = 10$, the same error in energy level ($1\,{\rm cm}^{-1}$) results in a error in quantum defects about 0.004.

Noted that related to $4s^2nfJ^\pi = (7/2)^\circ$ series, there are 38 open or 'weakly' closed channels constructed on the first 14 Sc^+ levels as shown in Table 1, the 'weakly' closed channels mean that their precursor states are below or in the energy region of our target series. However, the angular change of the corresponding ionic core (except for the core $4s^2$ itself) compared to $4s^2$ is larger than 1, which means that these channels have multipole polarization effects on the $4s^2nfJ^\pi = (7/2)^\circ$ series. As a comparison, only these 38 channels entered calculations, the calculated quantum defects are denoted as μ_4. From the transformation matrices $U_{i\alpha}$, in which off-diagonal elements reflects channel–channel interactions, the off-diagonal elements of $U_{i\alpha}$ are much smaller than 1, and diagonal elements of $U_{i\alpha}$ are larger than 0.8 in the energy region of interest. Therefore, the calculated eigenquantum defect μ_4 is almost the same as the eigenquantum defect μ_2 obtained from FCA in the energy region of interest as shown Fig.1. This elucidates that dipole polarization effects play an important role on this autoionization Rydberg series $4s^2nfJ^\pi = (7/2)^\circ$, not the multipole polarization effects although these corresponding channels are open or 'weakly' closed channels.

Now we discuss the reason that the $4s^216f$ is obscured in experimental spectra. Figure 2 displays the calculated collision eigenphase shifts $\pi\tau_\rho$ for the $J^\pi = (7/2)^\circ$ resonances, in which 38 channels entered calculations. It is well known that the collision eigenphase shift $\pi\tau_\rho$ changes abruptly by π radians when the energy crosses the positions of the resonance states . As shown in Fig.2, the collision eigenphase $\pi\tau_\rho$ changes abruptly by 2π radians within $4\,{\rm cm}^{-1}$energy range, i.e., 64226-64230 $\rm cm^{-1}$ when energy crosses the position of $4s^216f$ resonance state. It means that there is another resonance state as well as $4s^216f$ resonance state in the 64226-64230 $\rm cm^{-1}$energy region. Such resonance state is converged to $3d^2(^1G_4)$ of Sc^+ based on our calculations. The configuration interaction between the two resonance states may be strong since the energy interval of this two resonance states is so small, and $4s^216f$ resonance state may be obscured by the perturbation. Such suggestion is consistent with the result of Greene *et al.*[3]

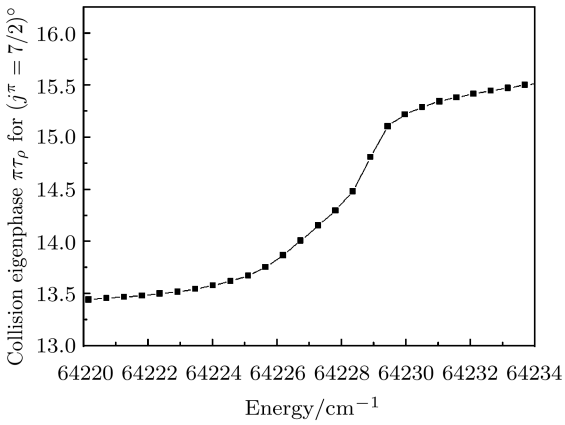


Fig.2. Collision eigenphase shifts $\pi\tau_\rho$ for the $J^\pi = (7/2)^\circ$ resonance states.

4. Conclusion

Based on RMCT and within the framework of MQDT, the energy levels of autoionization Rydberg series $4s^2nf(n = 4-23)J^\pi = (7/2)^\circ$ of scandium are calculated at different levels of approximation, i.e., self-consistent method, one channel calculations (i.e., frozen core approximation), five channels calculations by considering dipole polarization effects, 38 channels calculations by considering multipole polarization effects. As shown in Fig.1 and Table 2, the effects of dipole polarizations of $4s^2$ as 4s4p play an important role on autoionization Rydberg series

$4s^2nf(n = 4 - 23)J^\pi = (7/2)^\circ$, and the difference between experimental and calculated quantum defects for this series is generally about 0.01–0.03 with the exception of $n = 20, 22, 23$ as shown in Table 2. Furthermore, the reason that $4s^2 16f$ is obscured in experimental spectra is suggested to be the interaction with the neighbouring resonance state converged to $3d^2(^1G_4)$ of Sc^+ as shown in Fig.2.

Acknowledgments

The authors are deeply grateful to Professor Li Jia-Ming for helpful discussions.

References

[1] Russell H N and Ward J F 1927 *Scient. Pap. U. S. Bur. Stand.* **22** 329
[2] Kaufman V and Sugar J 1988 *J. Phys. Chem. Ref. Data* **17** 1679
[3] Robicheaux F and Greene C H 1993 *Phys. Rev.* A **48** 4429
Robicheaux F and Greene C H 1993 *Phys. Rev.* A **48** 4441
[4] Ding J, Yang Q H, Tang Z F, Xu J and Su L B 2007 *Acta Phys. Sin.* **56** 2207 (in Chinese)
[5] Jin Zh, Nie Q H, Xu T F, Dai Sh X, Shen X and Zhang X H 2007 *Acta Phys. Sin.* **56** 2261 (in Chinese)
[6] Garton W R S, Reeves E M, Tomkins F S and B Ercoli 1973 *Proc. R. Soc. London.* Ser. A **333** 1
[7] Robicheaux F and Greene C H 1993 *Phys. Rev.* A **47** 4908
[8] Robicheaux F and Greene C H 1991 *Phys. Rev.* A **44** 1773
[9] Rau A R P and Fano U 1971 *Phys. Rev.* A **4** 1751
[10] Lee C M and Lu K T 1973 *Phys. Rev.* A **8** 1241
[11] Lee C M (Li J M) and Johnson W R 1980 *Phys. Rev.* A **22** 979
[12] Seaton M J 1983 *Rep. Prog. Phys.* **46** 167
[13] Li J M 1980 *Acta Phys. Sin.* **29** 419 (in Chinese)
[14] Li J M 1983 *Acta Phys. Sin.* **32** 84 (in Chinese)
[15] Zou Y, Tong X M and Li J M 1995 *Acta Phys. Sin.* **44** 50 (in Chinese)
[16] Huang W, Zou Y, Tong X M and Li J M 1995 *Phys. Rev.* A **52** 2770
[17] Li J M, Wu Y J and Pratt R H 1989 *Phys. Rev.* A **40** 3036
[18] Yan J, Zhang P H, Tong X M and Li J M 1996 *Acta Phys. Sin.* **45** 1978 (in Chinese)
[19] Xia D and Li J M 2001 *Chin. Phys. Lett.* **18** 1334
[20] Xia D, Zhang S Zh, Peng Y L and Li J M 2003 *Chin. Phys. Lett.* **20** 56
[21] Lee C M (Li J M) 1974 *Phys. Rev.* A **10** 3036
[22] Libermann D A, Comer D T and Waber J T 1971 *Comp. Phys. Commun.* **2** 107
[23] Li J M and Zhao Z X 1981 *Acta Phys. Sin.* **30** 105 (in Chinese)